

Phase delay of polarisation modes in elastically twisted spun fibres

S.K. Morshnev, Yu.K. Chamorovsky, I.L. Vorob'ev

Abstract. The evolution of the phase delay between linearly polarised orthogonal modes in a spun fibre elastically twisted around its axis has been studied experimentally and theoretically using a model for a helical structure of the built-in linear birefringence axes. The phase delay is a sinusoidal function of elastic twist angle, with an amplitude and period dependent on fibre parameters: spin pitch and built-in linear birefringence beat length. It is shown that, at a known spin pitch, phase delay versus elastic twist angle data can be used to determine the beat length of built-in linear birefringence in the range 0.01 to 100 mm. The theoretical analysis results are supported by experimental data for conventional and microstructured spun fibres.

Keywords: optical fibre, spun fibre, helical structure of linear birefringence axes, phase delay.

1. Introduction

Spun fibre, fabricated by spinning a preform with a built-in linear birefringence (BR) during the drawing process, has been known since 1989 [1] and is used e.g. in magnetic-field and electric-current sensors [2–4]. Recent work [4–7] has shown that spun fibre has no built-in circular BR and that its properties are governed by the helical structure of its linear BR axes, which develops during the fibre drawing process.

The purpose of this report is to further study the properties of spun fibre, in particular its response to elastic twist. Elastic twist is known to influence the spin pitch of the helical structure of linear BR and to produce circular BR [8].

The study of the effect of elastic twist angle on the phase delay, R , between two polarisation modes in spun fibre may provide additional information about parameters of such fibre, in particular about the beat length of built-in linear BR.

2. Theory

As shown previously [4], the properties of a straight fibre with a helical structure of its built-in linear birefringence

axes can be described in a linear polarisation basis using the Jones matrix [9]

$$T \equiv \begin{vmatrix} T_{11} & T_{12} \\ T_{21} & T_{22} \end{vmatrix} = \frac{1}{\Omega} \begin{vmatrix} a_{11} + ib_{11} & a_{12} + ib_{12} \\ -a_{12} + ib_{12} & a_{11} - ib_{11} \end{vmatrix}, \quad (1)$$

where

$$\begin{aligned} a_{11} &= \Omega \cos \xi z \cos \Omega z + \left(\xi + \frac{\gamma}{2} \right) \sin \xi z \sin \Omega z; \\ a_{12} &= -\Omega \sin \xi z \cos \Omega z + \left(\xi + \frac{\gamma}{2} \right) \cos \xi z \sin \Omega z; \end{aligned} \quad (2)$$

$$b_{11} = \frac{\Delta\beta}{2} \cos \xi z \sin \Omega z;$$

$$b_{12} = \frac{\Delta\beta}{2} \sin \xi z \sin \Omega z;$$

$\Delta\beta = 2\pi/L_b$ is the rate at which the phase delay between waves with orthogonal linear polarisations increases with fibre length, z , because of the built-in linear BR with a beat length L_b ; $\gamma = 2\pi/L_c$ is the rate at which the phase delay between waves with orthogonal circular polarisations increases because of the circular BR with a beat length L_c ; $\xi = 2\pi/L_{tw}$ is the angular rotation rate of the helical structure of the built-in linear BR axes with a spin pitch L_{tw} ; and

$$\Omega = \sqrt{\left(\frac{\Delta\beta}{2} \right)^2 + \left(\xi + \frac{\gamma}{2} \right)^2} \quad (3)$$

is the spatial frequency.

An elastic twist of a straight fibre of length z by angle φ in the twist direction of the helical structure of the BR axes increases its angular rotation rate:

$$\xi = \frac{2\pi}{L_{tw}} + \frac{\varphi}{z} \equiv \xi_0 + \frac{\varphi}{z}. \quad (4)$$

A twist in the opposite direction ($\varphi < 0$) reduces ξ . Moreover, as shown by Rashleigh [8] the fibre acquires circular BR,

$$\gamma = \frac{\varphi}{\mu z}, \quad (5)$$

S.K. Morshnev, Yu.K. Chamorovsky, I.L. Vorob'ev Kotel'nikov Institute of Radio Engineering and Electronics (Fryazino Branch), Russian Academy of Sciences, pl. Vvedenskogo 1, 141190 Fryazino, Moscow region, Russia; e-mail: m137@fryazino.net, yuchamor@online.ru

Received 3 February 2011

Kvantovaya Elektronika 41 (5) 469–474 (2011)

Translated by O.M. Tsarev

where $\mu = 6.85$ for silica fibres. Physically, this means that, in a fibre of length z , one can obtain circular BR with a beat length $L_c = z$ by making about seven turns around the fibre axis over a length L_c .

A phase delay, R , between waves with orthogonal linear polarisations is known to result in an elliptic state of the field, with an ellipticity angle ε ($R = 2\varepsilon$) [9]. Ellipticity, defined as the ratio of the semiminor axis (b) to the semimajor axis (a) of the polarisation ellipse, is related to the ellipticity angle by $\tan \varepsilon = \pm b/a$. In a fibre with linear birefringence (without twist), the phase delay between waves with orthogonal linear polarisations increases in proportion to fibre length. In spun fibres, the phase delay varies between its maximum and minimum values along the fibre length [10].

Consider the polarisation state evolution in the complex plane [9] where the coordinates of points, χ , are the ratios of the orthogonal components E_x and E_y of the field:

$$\chi = u + iv = \frac{E_y}{E_x}. \quad (6)$$

This complex plane is a geodesic projection of the Poincare sphere. Its north pole (right-hand circular polarisation) projects onto the point $\{u, v\} = \{0, +i\}$, and its south pole (left-hand circular polarisation), onto the point $\{0, -i\}$. The equator of the Poincare sphere (all possible linear polarisations) projects onto the real axis. In particular, $E\|x$ projects onto the point $\{0, 0\}$, and $\{\infty, \infty\}$ corresponds to $E\|y$. The latitude of a point corresponds to the phase delay, and its longitude, to twice the azimuth angle of the elliptic state [9]. Using notation (2), we obtain

$$\chi = \frac{(-a_{12}E_{x0} + a_{11}E_{y0}) + i(b_{12}E_{x0} - b_{11}E_{y0})}{(a_{11}E_{x0} + a_{12}E_{y0}) + i(b_{11}E_{x0} + b_{12}E_{y0})}. \quad (7)$$

We consider linearly polarised states at the fibre input that differ only in azimuth, α :

$$E_{x0} = E_0 \cos \alpha, \quad E_{y0} = E_0 \sin \alpha. \quad (8)$$

Substituting (2) and (8) into (7), we find χ as a function of fibre length. Such dependences, differing in the azimuth of the linear polarisation of light at the fibre input and in linear birefringence, $\Delta\beta$, are presented in Figs 1 and 2, respectively.

As seen in Fig. 1a, excitation at the $E\|x$ polarisation ($\alpha = 0$) causes the largest deviation of the polarisation state from the equator of the Poincare sphere, i.e., the largest phase delay, roughly equal to the peak-to-peak amplitude of the nearly sinusoidal phase delay oscillations in Fig. 1b. It is worth pointing out that the rise in the oscillation amplitude at the left and right of Figs 1a and 1b, respectively, is simply a distortion related to the projection of the sphere onto the plane.

It is clear from Figs 1 and 2 that the helical structure of the linear BR axes ensures rotation of the plane of polarisation, with a polarisation state evolution from right to left along the equator of the Poincare sphere, even though there is no built-in circular BR (see Morshnev et al. [7] for more details). Comparison of Figs 2a and 2b indicates that the increase in built-in linear BR (decrease in L_b) is accompanied by an increase not only in the largest phase delay but also in the azimuthal rotation rate of the plane of polar-

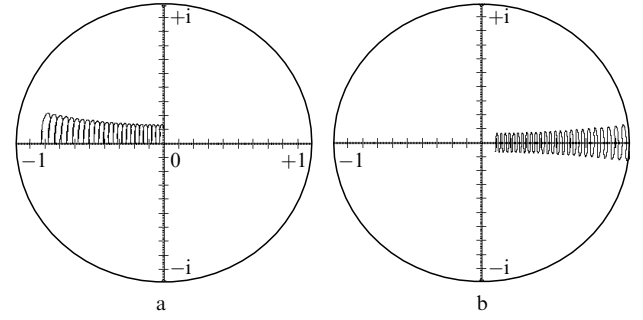


Figure 1. Polarisation state evolution (from right to left) along a spun fibre as represented in the complex plane: $L_b = 15$ mm, $L_{tw} = 4$ mm, $z = 50$ mm, azimuth of the linear polarisation of light at the fibre input $\alpha =$ (a) 0 and (b) 45° .

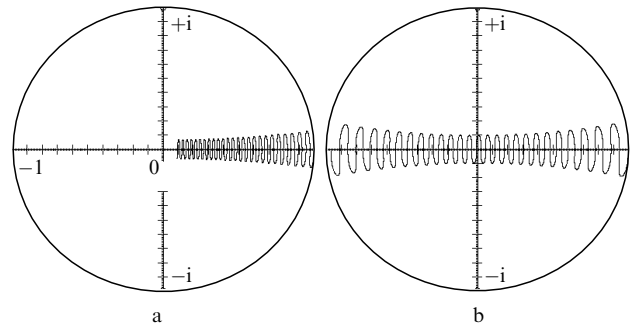


Figure 2. Polarisation state evolution (from right to left) along a spun fibre as represented in the complex plane: $L_{tw} = 4$ mm, $z = 50$ mm, $\alpha = 45^\circ$, $L_b =$ (a) 15 and (b) 10 mm.

isation. Thus, the rotation of the plane of polarisation is due to the built-in linear BR with a helical structure of its axes. The phase delay is a periodic function of fibre length, z , with a spatial period $L_{tw}/2$, which is ~ 2 mm in our case. This adds complexity to phase delay measurements because the phase delay, R , may drop from its maximum to minimum value over a fibre length within ~ 1 mm.

The exact value of R at the output of a fibre of length z is given by [9]

$$\sin R = \frac{2\text{Im}\chi}{1 + \chi^2}. \quad (9)$$

Using relation (7), we obtain for a spun fibre

$$\sin R = 2 \frac{(E_{x0}^2 - E_{y0}^2)(a_{11}b_{12} + a_{12}b_{11})}{\Omega^2 E_0^2} + 2 \frac{2E_{x0}E_{y0}(a_{12}b_{12} - a_{11}b_{11})}{\Omega^2 E_0^2}. \quad (10)$$

Substituting (2) and (8) into (10) and performing trigonometric transformations, we find

$$\sin R = \frac{\Delta\beta (\xi + \gamma/2)(1 - \cos 2\Omega z) \cos 2\alpha - \Omega \sin 2\Omega z \sin 2\alpha}{2 \Omega^2}. \quad (11)$$

It is clear from (11) that the phase delay is due to the built-in linear BR ($\Delta\beta/2$ factor) and is a periodic function of fibre length, z . At a given value of z , one can obtain

periodic variations in phase delay between its minimum and maximum values by varying the spatial frequency, Ω , through elastic twist of the fibre around its axis. Indeed, it follows from (4) and (5) that elastic twist with an increase in $|\varphi|$ causes a monotonic variation in spin pitch and weak circular BR, changing the spatial frequency, Ω [see (3)]. The coefficients of the harmonic functions in (11) are insensitive to elastic twist.

In Fig. 3, the phase delay, R , calculated using Eqn (11) is plotted against elastic twist angle, φ , for a typical spun fibre with a beat length $L_b = 15$ mm and a spin pitch $L_{tw} = 4$ mm. It is seen in Fig. 3a that, when the polarisation at the fibre input is parallel to the x axis of the fibre ($\alpha = 0$), the elastic twist causes the phase delay to periodically vary from 0 to $\sim 15^\circ$. The oscillation period in terms of the twist angle is $\sim 180^\circ$. Similarly, if incident light is polarised at 45° to the linear BR axes at the fibre input ($\alpha = 45^\circ$), the phase delay varies periodically from about -7.5° to $+7.5^\circ$ (the same oscillation amplitude of 15°) with the same oscillation period as above.

Note that, in Fig. 3, the circular BR that results from twist is too weak to show up. This is due to the great length of the spun fibre under investigation, $z = 1$ m, so that a twist of seven turns leads to a circular BR beat length $L_c = 1$ m $\gg L_b$. At a spun-fibre length $z = 10$ cm, a twist of seven turns will markedly reduce the phase delay oscillation amplitude (by approximately 20%), but the circular BR will be still weak, and its beat length, $L_c = 10$ cm, will exceed the linear BR beat length, $L_b = 15$ mm.

Consider now relation (11). Let the input beam be linearly polarised along the x axis ($\alpha = 0$). Then $\sin 2\alpha = 0$, and an elastic twist of the spun fibre causes $\sin R$ to vary from zero to its maximum value [see (11)]:

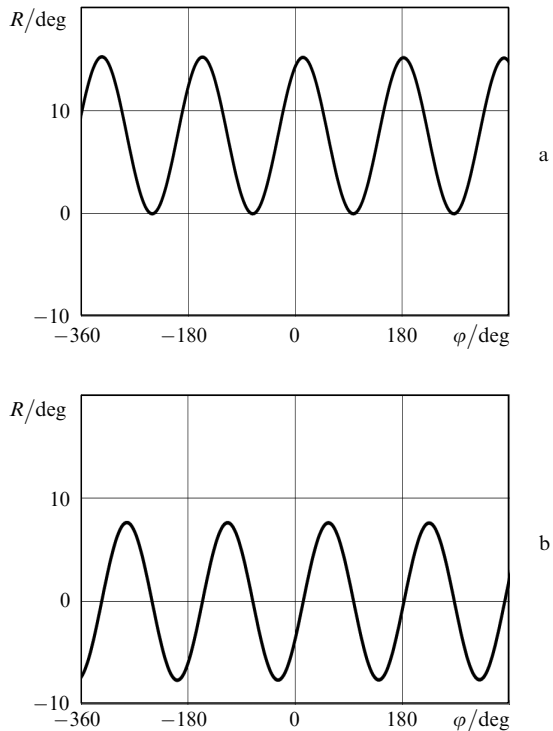


Figure 3. Phase delay R as a function of elastic twist angle φ for a 1-m-long spun fibre with a built-in linear BR: $L_b = 15$ mm, $L_{tw} = 4$ mm, $\alpha =$ (a) 0 and (b) 45° .

$$\sin R_{\max} = 2 \frac{\Delta\beta(\xi + \gamma/2)}{2\Omega^2} \approx \frac{4\xi_0\Delta\beta}{\Delta\beta^2 + 4\xi_0^2}, \quad (12)$$

where ξ_0 is the angular rotation rate in the absence of elastic twist [see (4)]. It follows from (12) that the maximum phase delay, R_{\max} , can reach $\pi/2$ only when $\Delta\beta = 2\xi_0$, i.e., when the beat length of the built-in linear BR is half the spin pitch: $L_b = L_{tw}/2$. At the same time, further increasing the built-in linear BR reduces the phase delay, as illustrated in Fig. 4.

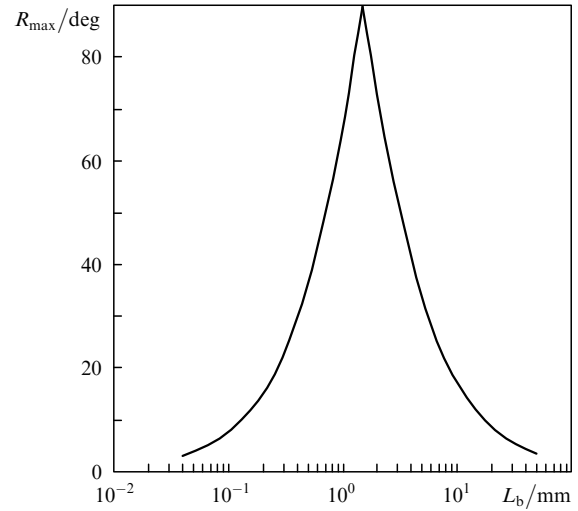


Figure 4. Maximum phase delay, R_{\max} , as a function of the beat length of built-in linear BR, L_b , for a spun fibre at $\alpha = 0$, $L_{tw} = 3$ mm and $z = 1$ m.

Thus, measuring the phase delay as a function of elastic twist angle, $R(\varphi)$ (Fig. 3), and determining the maximum phase delay from the peak-to-peak oscillation amplitude, one can find the beat length of the built-in linear BR in a rather wide range, from ~ 100 to ~ 0.1 mm, using Eqn (12). Note, however, that function (12) is ambiguous, and one should know whether the beat length L_b is greater or less than half the spin pitch, $L_{tw}/2$. In spun microstructured fibres, the beat length lies in the range $L_b < 0.1$ mm [11–13], where the procedure in question is inaccurate (see below).

Consider now the variation in oscillation period under such conditions. At a fibre length $z \sim 1$ m, the contribution of elastic twist to ξ_0 is not large [see (4) and (5)]: $\varphi/z + \varphi/(2\mu z) \ll \xi_0$. The spatial frequency Ω is given by

$$\begin{aligned} \Omega &\approx \sqrt{\left(\frac{\Delta\beta}{2}\right)^2 + \xi_0^2 + 2\xi_0\left(\frac{\varphi}{z} + \frac{\varphi}{2\mu z}\right)} \\ &\approx \Omega_0 \left[1 + \frac{\xi_0}{\Omega_0^2} \left(\frac{\varphi}{z} + \frac{\varphi}{2\mu z}\right)\right], \end{aligned} \quad (13)$$

where $\Omega_0^2 = (\Delta\beta/2)^2 + \xi_0^2$. The sine argument in (11) is

$$2\Omega z \approx 2\Omega_0 z + \frac{2\xi_0}{\Omega_0} \left(1 + \frac{1}{2\mu}\right) \varphi. \quad (14)$$

The oscillation period in terms of the elastic twist angle, $\Delta\varphi$, can be found by equating the second term on the right-hand side of (14) to 2π :

$$\Delta\varphi = \frac{\Omega_0}{\xi_0[1 + 1/(2\mu)]} \pi. \quad (15)$$

Knowing the spin pitch L_{tw} and experimentally determining $\Delta\varphi$, one can find the beat length of the built-in linearly BR from (15):

$$L_b = \frac{L_{tw}}{2\sqrt{[1 + 1/(2\mu)]^2(\Delta\varphi/\pi)^2 - 1}}. \quad (16)$$

For a spun microstructured fibre, we have $\Delta\beta \gg \xi_0$ and $\Omega_0 \approx \Delta\beta/2$. Therefore, the beat length is given by

$$L_b = \frac{L_{tw}}{2[1 + 1/(2\mu)]} \frac{\pi}{\Delta\varphi}. \quad (17)$$

Figure 5 shows the phase delay as a function of elastic twist angle at $\alpha = 45^\circ$, a fibre length $z = 1$ m, spin pitch $L_{tw} = 3$ mm and beat length $L_b = 0.075$ mm. As seen, the oscillation period of the phase delay, R , is about nine turns. Figure 6 plots $\Delta\varphi$ against the beat length of the built-in linear BR, L_b . The oscillation period $\Delta\varphi$ rises steeply with decreasing beat length L_b . In particular, $\Delta\varphi = 139.8\pi$, or ~ 69.9 turns, at $L_b = 0.01$ mm. As seen in Fig. 5, the oscillation period can be determined from the slope of the measured $R(\varphi)$.

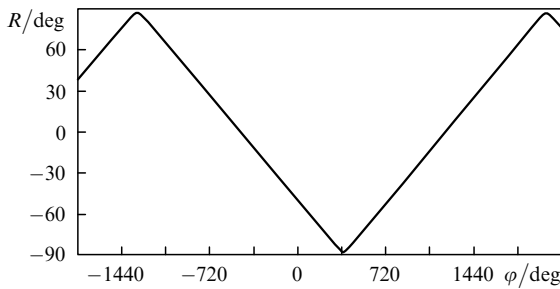


Figure 5. Phase delay R as a function of elastic twist angle φ for a 1-m-long spun fibre with a built-in linear BR: $L_b = 0.075$ mm, $L_{tw} = 3$ mm, $\alpha = 45^\circ$.

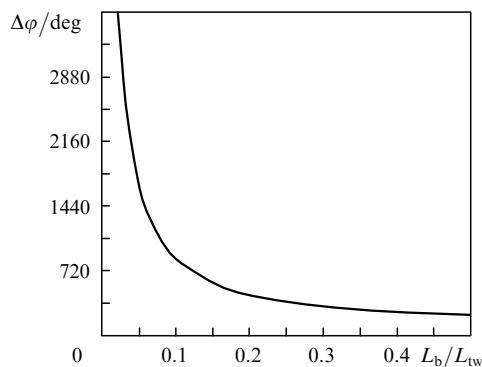


Figure 6. Elastic twist period $\Delta\varphi$ against the ratio of the beat length of built-in linear BR, L_b , to the spin pitch, L_{tw} , for spun fibre.

3. Experimental

Figure 7 schematically shows the experimental setup used. The light source is a 1.55- μm semiconductor laser (1)

energised from a stabilised current source (2). The parallel light beam formed by an objective (3) passes through a mechanical chopper (4) and linear polariser (5). Rotating the polariser changes the azimuth angle α relative to the linear BR axes at the fibre input. Another objective (6), with a positioning stage (7), focuses the beam onto the input end of a spun fibre (8) secured to the table (9) of a tensioner with an optical cement (10). Tension is applied through a filament thrown over a pulley (11) and is produced by a load of ~ 0.4 N (12). The fibre is twisted around its axis by a rotor (13), with the output fibre end secured to its table with an optical cement (10). The beam emerging from the output fibre end passes through an analyser (14) and is detected by a photodiode (15). The modulated photocurrent is fed to a lock-in amplifier (16), whose signal is measured by a digital voltmeter (17).

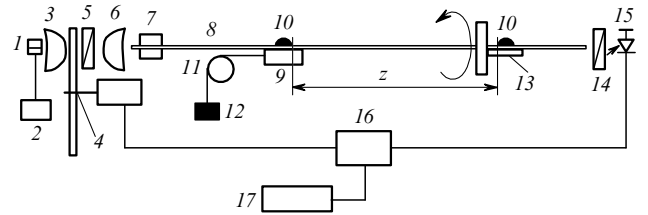


Figure 7. Schematic of the experimental setup for phase delay measurements: (1) light source (semiconductor laser), (2) laser power supply, (3) collimating objective, (4) mechanical chopper, (5) polariser, (6) objective for coupling the beam into fibre; (7) alignment system, (8) fibre, (9) table of the tensioner, (10) optical cement, (11) pulley, (12) load, (13) table of the rotation system, (14) analyser at the fibre output, (15) photodetector; (16) lock-in amplifier, (17) digital voltmeter.

The phase delay, R , can be found from the known relation

$$\cos R = \frac{I_{\max} - I_{\min}}{I_{\max} + I_{\min}}, \quad (18)$$

where I_{\max} and I_{\min} are the intensities obtained by rotating the analyser (14) and characterising the ellipticity of the output beam at zero dichroism of the fibre.

To check the above theoretical analysis, we studied a spun fibre with a known built-in linear BR: beat length $L_b = 15 \pm 1$ mm [14] and spin pitch $L_{tw} = 3.5$ mm. Our experimental data are presented in Fig. 8. The difference between the maximum and minimum phase delay is $13^\circ \pm 0.2^\circ$. From (12), we then obtain $L_b = 15.3 \pm 0.3$ mm.

An interesting distinction of the experimental data from theoretical predictions (Fig. 3a) is that the $R(\varphi)$ curve is elevated over the abscissa, which may be due to the effect of the fibre segment between the alignment stage (7) and the point where the fibre is secured to the table (9) of the tensioner. The length of this fibre segment (which is obviously untwisted) was 40 cm. The solid curve in Fig. 8 was calculated with allowance for this fibre segment. As seen, the calculation results for a beat length $L_b = 15.2$ mm agree well with the experimental data.

Note that five turns do not change the phase delay oscillation amplitude. This means that the effect of twist-induced circular BR is negligible and that there is no built-in circular BR in the fibre.

Figure 9 presents experimental data for a spun microstructured fibre [12, 13] with a built-in BR beat length less

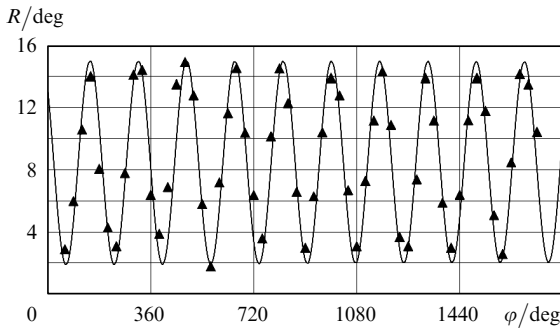


Figure 8. Calculated phase delay R as a function of elastic twist angle φ (solid curve) for a spun fibre of length $z = 1$ m with a beat length of built-in linear BR $L_b = 15.2$ mm and a spin pitch $L_{tw} = 3.5$ mm. The solid triangles represent the experimental data.

than its spin pitch: $L_b \sim 1$ mm, $L_{tw} = 3$ mm. The phase delay (peak-to-peak amplitude in Fig. 9) is $R = 62^\circ$. As apparent from Fig. 4, determining the beat length from the phase delay [Eqn (12)] we obtain two values: $L_b \approx 0.9$ and 3 mm. It is worth while to verify this result using elastic twist period measurements. The measured $\Delta\varphi$ in the fibre is 286° . From (17), we obtain $L_b \approx 1.08$ mm. Thus, starting at a beat length $L_b \sim 1$ mm, elastic twist period measurements give more accurate L_b values.

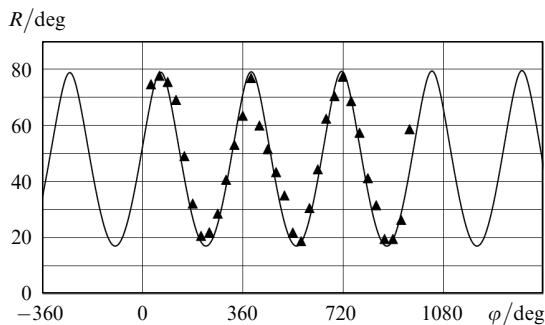


Figure 9. Calculated phase delay R as a function of elastic twist angle φ (solid curve) for a spun fibre of length $z = 1$ m with a beat length of built-in linear BR $L_b = 0.9$ mm and a spin pitch $L_{tw} = 3$ mm. The solid triangles represent the experimental data.

The proposed procedure for measuring the beat length of built-in linear BR in spun fibres was applied to a spun microstructured fibre with a high built-in linear BR. The measurement results are presented in Fig. 10. The experimentally determined $\Delta\varphi$ of this fibre is 525° . From (17), we obtain $L_b = 0.5$ mm. It is worth pointing out that the oscillation amplitude is substantially smaller than that predicted theoretically. The fibre length was ~ 1.5 m, and the depolarisation properties of spun fibre might play a significant role [15]. Indeed, the injection laser used in the measurements had an emission bandwidth of ~ 0.1 nm. According to earlier estimates [15], this gives a coherence length of ~ 3.7 m at $L_b = 0.5$ mm.

It may be that depolarisation also influenced the results for the previous fibre: the L_b estimated from the phase delay oscillation amplitude ($L_b \approx 0.9$ mm) is smaller than that estimated from the elastic twist period ($L_b \approx 1.08$ mm), which can be accounted for by partial depolarisation.

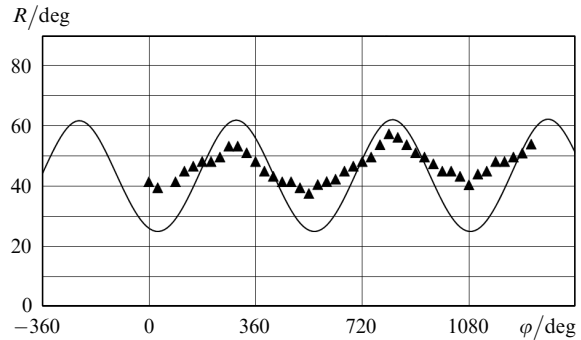


Figure 10. Calculated phase delay R as a function of elastic twist angle φ (solid curve) for a spun fibre of length $z = 1$ m with a beat length of built-in linear BR $L_b = 0.48$ mm and a spin pitch $L_{tw} = 3$ mm. The solid triangles represent the experimental data.

4. Conclusions

The behaviour of the phase delay between linearly polarised orthogonal modes in a spun fibre elastically twisted around its axis is consistent with theoretical analysis in terms of the helical structure of built-in linear BR [4–7]. According to this theoretical interpretation, the fibre has no built-in circular BR. A weak circular BR only results from an elastic twist of the fibre around its axis. This is supported by experimental data.

The beat length of built-in linear BR in a spun fibre can be determined experimentally both from the phase delay oscillation amplitude as a function of elastic twist angle and from the oscillation period.

Beat length determination from the oscillation amplitude has the following drawbacks:

1. At a beat length L_b small compared to the spin pitch L_{tw} , there is an ambiguity in L_b determination (Fig. 4).
2. At low L_b values, the fibre length necessary for measurements is comparable to the coherence length of the light source, which contributes to the error of L_b determination (depolarisation reduces the phase delay oscillation amplitude).

A drawback to L_b determination from the phase delay oscillation period is that, at great beat lengths ($L_b > 10$ mm), the oscillation period is a weak function of L_b and this approach is less accurate than L_b determination from the oscillation amplitude.

Combining the two approaches, one can determine the beat length of built-in linear BR in spun fibres in a wide range: from ~ 0.01 to ~ 100 mm.

References

1. Laming R.I., Payne D.N. *J. Lightwave Technol.*, **7**, 2084 (1989).
2. Blake J., Tantaswadi P., de Carvalho A. *IEEE Trans. Power Delivery*, **11**, 116 (1996).
3. Short S.X., Tselikov A.A., de Arruda J.U., Blake J.N. *J. Lightwave Technol.*, **16**, 1212 (1998).
4. Gubin V.P., Isaev V.A., Morshnev S.K., Sazonov A.I., Starostin N.I., Chamorovsky Yu.K., Oussov A.I. *Kvantovaya Elektron.*, **36**, 287 (2006) [*Quantum Electron.*, **36**, 287 (2006)].
5. Morshnev S.K., Gubin V.P., Isaev V.A., Starostin N.I., Chamorovsky Yu.K. *Foton-Ekspress*, **6**, 64 (2007).
6. Morshnev S.K., Gubin V.P., Isaev V.A., Starostin N.I., Sazonov A.I., Chamorovsky Yu.K., Korotkov N.M. *Opt. Mem. Neural Networks*, **17**, 258 (2008).

7. Morshnev S.K., Gubin V.P., Vorob'ev I.L., Starostin N.I., Sazonov A.I., Chamorovsky Yu.K., Korotkov N.M. *Kvantovaya Elektron.*, **39**, 287 (2009) [*Quantum Electron.*, **39**, 287 (2009)].
8. Rashleigh S.C. *J. Lightwave Technol.*, **1**, 312 (1983).
9. Azzam R.M.A., Bashara N.M. *Ellipsometry and Polarized Light* (Amsterdam: North-Holland, 1977; Moscow: Mir, 1981).
10. Aksenov V.A., Morshnev S.K., Ivanov G.A., Chamorovsky Yu.K. *Sbornik trudov 13-i mezhdunarodnoi nauchnoi konf. MMTT-2000 (Proc. 13th Int. Conf. Mathematical Methods in Engineering and Technology, MMET-2000)* (St. Petersburg, 2000) Vol. 7, p. 53.
11. Michie A., Canning J., Bassett J., Haywood J., Digweed K., Aslung M., Ashton B., Stevenson M., Digweed J., Lau A., Scandurra D. *Opt. Express*, **15**, 1811 (2007).
12. Chamorovsky Yu.K., Starostin N.I., Ryabko M.V., Sazonov A.I., Morshnev S.K., Gubin V.P., Vorob'ev I.L., Nikitov S.A. *Opt. Commun.*, **282**, 4618 (2009).
13. Chamorovsky Yu.K., Starostin N.I., Morshnev S.K., Gubin V.P., Ryabko M.V., Sazonov A.I., Vorob'ev I.L. *Kvantovaya Elektron.*, **39**, 1074 (2009) [*Quantum Electron.*, **39**, 1074 (2009)].
14. Morshnev S.K., Ryabko M.V., Ghamorovsky Yu.K. *Proc. SPIE Int. Soc. Opt. Eng.*, **6594**, 6594OR (2007).
15. Gubin V.P., Morshnev S.K., Starostin N.I., Sazonov A.I., Chamorovsky Yu.K., Isaev V.A. *Radiotekh. Elektron.*, **53**, 971 (2008).